Planta (2019) 249:527–542
https://doi.org/10.1007/s00425-018-3024-5

ORIGINAL ARTICLE

Characterization of Maf1 in *Arabidopsis*: function under stress conditions and regulation by the TOR signaling pathway

Chang Sook Ahn[1,2] · **Du-Hwa Lee**[1] · **Hyun-Sook Pai**[1]

Received: 14 August 2018 / Accepted: 30 September 2018 / Published online: 6 October 2018

Abstract

Main conclusion **Maf1 repressor activity is critical for plant survival during environmental stresses, and is regulated by its phosphorylation/dephosphorylation through the activity of TOR and PP4/PP2A phosphatases.**

Maf1 is a global repressor of RNA polymerase III (Pol III), and is conserved in eukaryotes. Pol III synthesizes small RNAs, 5S rRNA, and tRNAs that are essential for protein translation and cell growth. Maf1 is a phosphoprotein and dephosphorylation of Maf1 promotes its repressor activity in yeast and mammals. Plant Maf1 was identified in citrus plants as a canker elicitor-binding protein, and citrus Maf1 represses cell growth associated with canker development. However, functions of plant Maf1 under diverse stress conditions and its regulation by the target of rapamycin (TOR) signaling components are poorly understood. In this study, the *Arabidopsis maf1* mutants were more susceptible to diverse stresses and treatment with the TOR inhibitor Torin-1 than wild-type plants. The *maf1* mutants expressed higher levels of Maf1 target RNAs, including 5S rRNA and pre-tRNAs in leaf cells, supporting Pol III repressor activity of *Arabidopsis* Maf1. Cellular stresses and Torin-1 treatment induced dephosphorylation of Maf1, suggesting Maf1 activation under diverse stress conditions. *TOR* silencing also stimulated Maf1 dephosphorylation, while silencing of catalytic subunit genes of PP4 and PP2A repressed it. Thus, TOR kinase and PP4/PP2A phosphatases appeared to oppositely modulate the Maf1 phosphorylation status. *TOR* silencing decreased the abundance of the target RNAs, while silencing of the PP4 and PP2A subunit genes increased it, supporting the positive correlation between Maf1 dephosphorylation and its repressor activity. Taken together, these results suggest that repressor activity of Maf1, regulated by the TOR signaling pathway, is critical for plant cell survival during environmental stresses.

Keywords Phosphorylation/dephosphorylation · Phos-tag gels · Protein phosphatases · Target gene expression · TOR · Virus-induced gene silencing

Introduction

The target of rapamycin (TOR) is a central metabolic sensor conserved in all eukaryotes, which coordinates cell proliferation and growth in response to diverse signals, including nutrient availability, growth factors, energy status, and environmental conditions (Wullschleger et al. 2006; Bögre et al. 2013; Xiong and Sheen 2013; Dobrenel et al. 2016). Under favorable conditions, TOR is activated to promote anabolic processes such as transcription, ribosome biogenesis, and protein synthesis. However, unfavorable conditions such as nutrient deficiency and environmental stresses inactivate TOR to promote autophagy, proteolysis, and stress responses. Particularly, TOR is the master regulator of ribosome biogenesis and mRNA translation, acting through

Electronic supplementary material The online version of this article (https://doi.org/10.1007/s00425-018-3024-5) contains supplementary material, which is available to authorized users.

✉ Hyun-Sook Pai
hspai@yonsei.ac.kr

Chang Sook Ahn
soogi77s@nate.com

Du-Hwa Lee
niroo@yonsei.ac.kr

[1] Department of Systems Biology, Yonsei University, Seoul 03722, Korea

[2] Present Address: Future Technology Research Center, Corporate R&D, LG Chem/LG Science Park, Seoul 07796, Korea

the regulation of transcription network and phosphorylation of translation machinery (Wullschleger et al. 2006; Ma and Blenis 2009; Thoreen et al. 2012; Schepetilnikov et al. 2013).

TOR has been implicated in the control of RNA polymerase I-mediated transcription of ribosomal RNAs, which is essential for ribosome biogenesis and cell mass accumulation (Hannan et al. 2003; Mayer and Grummt 2006). Furthermore, previous studies suggested that the TOR pathway regulates RNA polymerase III-dependent transcription in a nutrient-dependent way (Zaragoza et al. 1998; Lee et al. 2009; Wei et al. 2009). RNA polymerase III (Pol III) synthesizes small non-coding RNAs including 5S rRNA, tRNAs, and U6 snRNA that are involved in translation, splicing, and various other processes (Dieci et al. 2007; White 2008). Nutrient deficiency and stress conditions repress global protein synthesis activity, accompanied by repression of Pol III activity via multiple signaling pathways, including the TOR signaling pathway (Wei and Zheng 2010; Boguta 2012).

Maf1 is a global Pol III repressor, conserved in eukaryotes. Maf1 represses Pol III transcription in response to starvation, rapamycin treatment, DNA damage, and oxidative stress by direct interaction with the Pol III machinery (Pluta et al. 2001; Upadhya et al. 2002; Reina et al. 2006; Boisnard et al. 2009). Maf1 interacts with the Pol III components including Rpc160, and with the TFIIIB component Brf1, blocking the recruitment of Pol III to the TFIIIB-TFIIIC-DNA complexes (Desai et al. 2005; Rollins et al. 2007; Vannini et al. 2010). Maf1 exists in various phosphorylation states, and Pol III repression requires Maf1 in a dephosphorylated state in yeast (Moir et al. 2006; Oficjalska-Pham et al. 2006; Roberts et al. 2006; Lee et al. 2009; Wei et al. 2009; Boguta 2012). In favorable growth conditions, Maf1 is inactivated by phosphorylation, which decreases direct binding of Maf1 to Pol III, and promotes Maf1 export from the nucleus to the cytosol. Recent studies in yeast suggested that phosphorylation is the key mechanism for controlling Maf1 activity, while the nuclear-cytoplasmic transport of Maf1 may be a fine-tuning mechanism (Boguta 2012). Mammalian Maf1, being predominantly nuclear localized, is also mainly regulated by phosphorylation. Human Maf1 becomes dephosphorylated after serum starvation, methyl methanesulfonate (MMS) or rapamycin treatment, leading to its association with Pol III (Reina et al. 2006; Goodfellow et al. 2008; Boguta 2012).

Based on recent reports, yeast Maf1 is phosphorylated at different sites by multiple kinases, including protein kinase A (PKA), Sch9 (S6K homolog), TOR complex 1 (TORC1), and casein kinase 2 (CK2) in response to favorable conditions (Moir et al. 2006; Lee et al. 2009; Wei et al. 2009; Graczyk et al. 2011). However, it is still not known how Maf1 phosphorylation by each of those kinases contributes to the control of Maf1 interaction with Pol III. In mammalian cells, Maf1 is phosphorylated by mammalian TOR (mTOR) and CK2 that are associated with the promoters of tRNA and 5S rRNA genes (Kantidakis et al. 2010; Michels et al. 2010; Boguta and Graczyk 2011). Phosphorylated Maf1 is released from chromatin and dissociated from the Pol III complex. Therefore, these kinases antagonize Maf1 repression of Pol III, partly by inhibiting association of Maf1 with Pol III at Pol III target genes. Maf1 is rapidly dephosphorylated under stress. PP2A phosphatase has been implicated in Maf1 dephosphorylation in yeast. A triple mutation of PP2A catalytic subunit genes (*pph21*Δ *pph22-ts pph3*Δ) impairs Maf1 dephosphorylation and Pol III repression (Oficjalska-Pham et al. 2006). However, a more recent study suggested that PP4 phosphatase complex including Pph3 as its catalytic subunit plays a main role in Maf1 dephosphorylation in response to diverse stresses (Oler and Cairns 2012). However, the identity of phosphatase complexes that dephosphorylate Maf1 remains unclear in other systems.

Citrus Maf1 (CsMAF1) was identified as a PthA4-interacting protein; PthA4 is a transcription activator-like effector of citrus canker pathogen *Xanthomonas citri* (Soprano et al. 2013). CsMAF1 binds to human Pol III, and can suppress $tRNA^{His}$ expression in yeast. Silencing of *CsMAF1* leads to higher accumulation of tRNAs and elevated canker symptoms, while overexpression of *CsMAF1* attenuated both tRNA synthesis and canker disease development (Soprano et al. 2013). The crystal structure of the globular core of CsMAF1 shows a conserved Maf1-fold (Soprano et al. 2017). CsMAF1 is phosphorylated by murine PKA in vitro. Auxin treatment and a mutation of the PKA phosphorylation site influence the subcellular localization of CsMAF1. CsMAF1 is also phosphorylated by human mTOR at conserved serine residues in vitro, and AZD8055, an mTOR inhibitor, suppressed canker development (Soprano et al. 2017). These results suggest that CsMAF1 is involved in the control of cell growth during canker development as a Pol III repressor, under the control of auxin and multiple kinases. However, plant Maf1 functions under diverse stress conditions and detailed mechanisms of Maf1 regulation are poorly understood. In this study, we analyzed the phenotypes and target RNA expression in *Arabidopsis maf1* mutants under diverse stresses and Torin-1 treatment. Furthermore, we examined in vivo phosphorylation of Maf1 using Phos-tag SDS–PAGE, under stress conditions and after silencing of the TOR signaling components. We discuss possible mechanisms of the function of plant Maf1 under stress conditions and their functional link with the TOR pathway.

Materials and methods

Plant materials and growth conditions

Arabidopsis thaliana ecotype Columbia-0 (Col-0) plants were grown in a growth room at 23 °C under a 16-h light/8-h dark cycle with 120 µmol/m^2 s light intensity. The *Arabidopsis maf1-1* (SALK_026637) and *maf1-2* mutant (SALK_054632) seeds were obtained from the *Arabidopsis* Biological Resource Center (ABRC). For the liquid culture, *Arabidopsis* seeds were surface sterilized and sown in six-well plates containing 1 ml of liquid medium (0.5 × Murashige-Skoog [MS] medium [Duchefa], pH 5.7) containing 30 mM glucose. *Nicotiana benthamiana* plants used for transient expression assays were grown in a growth room at 23 °C with 80 µmol/m^2 s light intensity under a 16-h light/8-h dark cycle.

Generation of *Arabidopsis* Maf1–Myc overexpression transgenic plants

To generate *Maf1* overexpression lines, the *Maf1* protein-coding sequence was cloned into the pCAMBIA-6xMyc vector. *Arabidopsis* (Col-0) plants were transformed by the floral dip method (Clough and Bent 1998), using *Agrobacterium* C58C1 strain. From more than 30 independent T_1 lines, seven T_2 lines were selected for T_3 propagation, based on gene expression levels. The seed batch showing 100% hygromycin resistance was selected as the homozygous T_3 generation. T_3 and T_4 homozygous seeds were used for the analyses.

Chlorophyll measurement

Chlorophyll was extracted from five seedlings in 80% aqueous acetone. Absorbance of the extract was measured at 663.6 and 646.6 nm using VersaMax Absorbance Microplate Reader (Molecular Devices). The total chlorophyll contents were calculated based on the absorbance, as described previously (Porra and Scheer 2000), and normalized by fresh weight.

Virus-induced gene silencing (VIGS)

VIGS was performed in *Arabidopsis* as previously described (Burch-Smith et al. 2006; Ahn et al. 2015b) using soil-grown plants at 2–4 leaf stages. Briefly, the wild-type (WT, Col-0) and OE-17 seeds were sown in soil, and at 10 days after germination, the largest true leaf of the plants was infiltrated with the *Agrobacterium* culture containing VIGS constructs using a needleless syringe. The VIGS phenotypes of the infiltrated plants were observed 15–18 days after infiltration (DAI). The ninth and tenth leaves, counting from the cotyledon, were collected from multiple VIGS plants for the RT-qPCR and Phos-tag SDS-PAGE analyses.

Stress treatment

Seedlings grown in liquid 1/2 MS medium containing 30 mM glucose for 7 days, were transferred to fresh medium containing H_2O_2 (40 and 80 mM), methyl methanesulfonate (MMS; 0.04%), and cisplatin (20 and 40 µM), and incubated for 24 or 48 h, as indicated. For stress treatment of VIGS plants (OE-17 background; 15 DAI), the ninth and tenth leaves were infiltrated with 40 mM H_2O_2 solution. After 24 h, the leaves were collected for the analyses.

Bimolecular fluorescence complementation (BiFC)

The *Maf1* coding region was PCR-amplified and cloned into the pSPYNE vector containing the N-terminal region of YFP (amino acid residues 1–155). Similarly, PPX1 and PP2Ac3 cDNAs were cloned into pSPYCE vector containing the C-terminal region of and yellow fluorescent protein (YFP; residues 156–239). The pSPYNE and pSPYCE fusion constructs were agroinfiltrated together into the leaves of 3-week-old *N. benthamiana* plants as described previously (Ahn et al. 2011). After 30 h, 40 mM H_2O_2, 0.04% MMS, and 50 µM cisplatin solution was infiltrated into the leaves that were previously agroinfiltrated. After 16 h, protoplasts were generated, and YFP signal was detected using a confocal microscope (Carl Zeiss LSM 700).

Reverse transcription-quantitative PCR (RT-qPCR)

Two micrograms of total RNA were used for cDNA synthesis using the RevertAid First Strand cDNA Synthesis Kit (Thermo Fisher Scientific) with oligo-dT or random primers according to the manufacturer's instructions. RT-qPCR was performed with diluted cDNAs (1:100) in 96-well plates using the RealHelix™ qRT-PCR Kit (NANOHELIX, Korea) and StepOnePlus Real-Time PCR System (Applied Biosystems) as described previously (Lee et al. 2017). *PP2AA3* and *UBC10* mRNAs were used as controls for normalization. The gene-specific primers used for RT-qPCR are listed in Table S1.

Phos-tag SDS-PAGE and immunoblotting

Protein sample preparation and Phos-tag SDS-PAGE were performed as described previously (Lee et al. 2017). The protein extracts were subjected to 8% Zn^{2+}-Phos-tag Bis–Tris NuPAGE with 50 µM $ZnCl_2$ and 50 µM Phos-taq system (Wako). After electrophoresis, the Phos-tag gels were

washed twice for 10 min each with transfer buffer (10 mM CAPS, pH 11) containing 10 mM EDTA to chelate the metal ions, followed by 10 min washing with transfer buffer without EDTA, and finally transferred onto polyvinylidene difluoride (PVDF) membranes for immunoblotting. Immunoblotting was performed with the anti-c-Myc-peroxidase antibody (Sigma-Aldrich; 1:10,000) and anti-Flag M2-HRP-conjugated antibody (Sigma-Aldrich; 1:10,000), according to the manufacturer's instructions. The signals were detected using Imagequant LAS 4000 (GE Healthcare Life Sciences).

Co-immunoprecipitation

6xMyc-fused constructs of Maf1, and 3xFlag-fused PPX1 and PP2Ac3 were transiently expressed in *N. benthamiana* by *Agrobacterium* infiltration. After the proteins were extracted with the protein extraction buffer, the Flag-fused proteins were immunoprecipitated using Anti-Flag M2 Affinity Gel (Sigma-Aldrich) according to the manufacturer's instruction. After elution of bead-bound proteins by boiling for 5 min, immunoblotting was performed with anti-c-myc-peroxidase antibody (Sigma-Aldrich; 1:10,000) and anti-Flag M2-HRP-conjugated antibody (Sigma-Aldrich; 1:10,000) for the detection of immunoprecipitated and co-immunoprecipitated proteins, respectively. The signals were detected using Imagequant LAS 4000 (GE Healthcare Life Sciences).

Results

Characterization of T-DNA insertion mutants and overexpression lines of *Maf1* in *Arabidopsis*

To investigate cellular functions of Maf1 in *Arabidopsis*, we obtained T-DNA tagging mutant lines (Col-0 ecotype) from ABRC. Two T-DNA insertion mutant lines were available for *Maf1* (At5g13240); *maf1-1* and *maf1-2* have a T-DNA insertion in the 2nd and 9th exons, respectively (Fig. 1a). Homozygous plants of *maf1-1* and *maf1-2* were selected based on genomic PCR (Fig. 1b, c). The *maf1-1* and *maf1-2* mutants did not express the full-length *Maf1* mRNA, based on RT-PCR (Fig. 1d). We also generated transgenic *Arabidopsis* lines (Col-0 ecotype) that constitutively express Maf1 fused to a 6xMyc tag (Maf1–Myc) under the control of cauliflower mosaic virus 35S promoter. The presence of *Maf1–Myc* transgene was confirmed by genomic PCR in more than 30 independent T_1 lines. Immunoblotting using anti-Myc antibody detected protein expression of the *Maf1–Myc* transgene in selected T_3 homozygous lines as a single band (Fig. S1a). Among these lines, OE-5 and OE-17 lines were selected for further analyses. RT-qPCR showed that OE-5 and OE-17 plants produced ~ 17- and ~ 14-fold higher levels of *Maf1* transcripts than the WT, respectively (Fig. 1e). Immunoblotting with anti-Myc antibody using leaf cell extracts confirmed the expression of Maf1–Myc protein in OE-5 and OE-17 lines (Fig. 1f). We observed overall growth and development of the T-DNA insertion mutants and OE lines of *Maf1*, compared with WT plants. Under optimal growth conditions, we observed no significant growth differences among these plants, suggesting that Maf1 deficiency or overexpression does not critically affect normal plant growth in soil.

Arabidopsis Maf1 proteins are localized in the nucleus and cytosol

To investigate the subcellular localization of *Arabidopsis* Maf1, we generated a green fluorescent protein (GFP) fusion construct of *Maf1* under the control of the *Maf1* promoter (2243 bp), designated *Maf1*p::Maf1–GFP (Fig. 1g). The construct was transiently expressed in *N. benthamiana* leaves via agroinfiltration. After 48 h, mesophyll protoplasts prepared from the infiltrated leaves were observed by confocal laser scanning microscopy. Maf1-GFP signals were mainly localized in the nucleus, but were also found in the cytosol, consistent with the localization of citrus Maf1 (Soprano et al. 2013).

The *maf1* mutants are more susceptible to diverse stresses than WT

To examine whether the *maf1* mutants and *Maf1* OE plants have any visible phenotypes under diverse stress conditions; we used the *Arabidopsis* liquid culture system. The WT, *maf1-1*, and *maf1-2* seedlings were grown in liquid 1/2 Murashige and Skoog (MS) medium with 30 mM glucose for 7 days, and then transferred to fresh medium without glucose, but containing H_2O_2 (40 and 80 mM), methyl methanesulfonate (MMS; 0.04%), and cisplatin (20 and 40 µM) (Fig. 2a). The seedlings were incubated under the stress conditions for 24 h (H_2O_2 and MMS) or 48 h (cisplatin). H_2O_2 induces oxidative stress (Apel and Hirt 2004). MMS damages DNA and RNA by alkylation (Revenkova et al. 1999; Lundin et al. 2005). Cisplatin, a chemotherapeutic drug, binds to DNA and inhibits its replication (Gately and Howell 1993). After stress treatment, total chlorophyll contents were measured from seedlings of each line to assess plant's resistance to the stresses (Fig. 2b). The WT, *maf1-1*, and *maf1-2* seedlings showed no differences in growth or total chlorophyll contents before treatment (control; CTR) (Fig. 2a, b). All seedlings stopped growth and lost chlorophyll after H_2O_2, MMS, and cisplatin treatment. However, the *maf1-1* and *maf1-2* mutant seedlings appeared to be more susceptible to all of these stresses than WT seedlings, based on

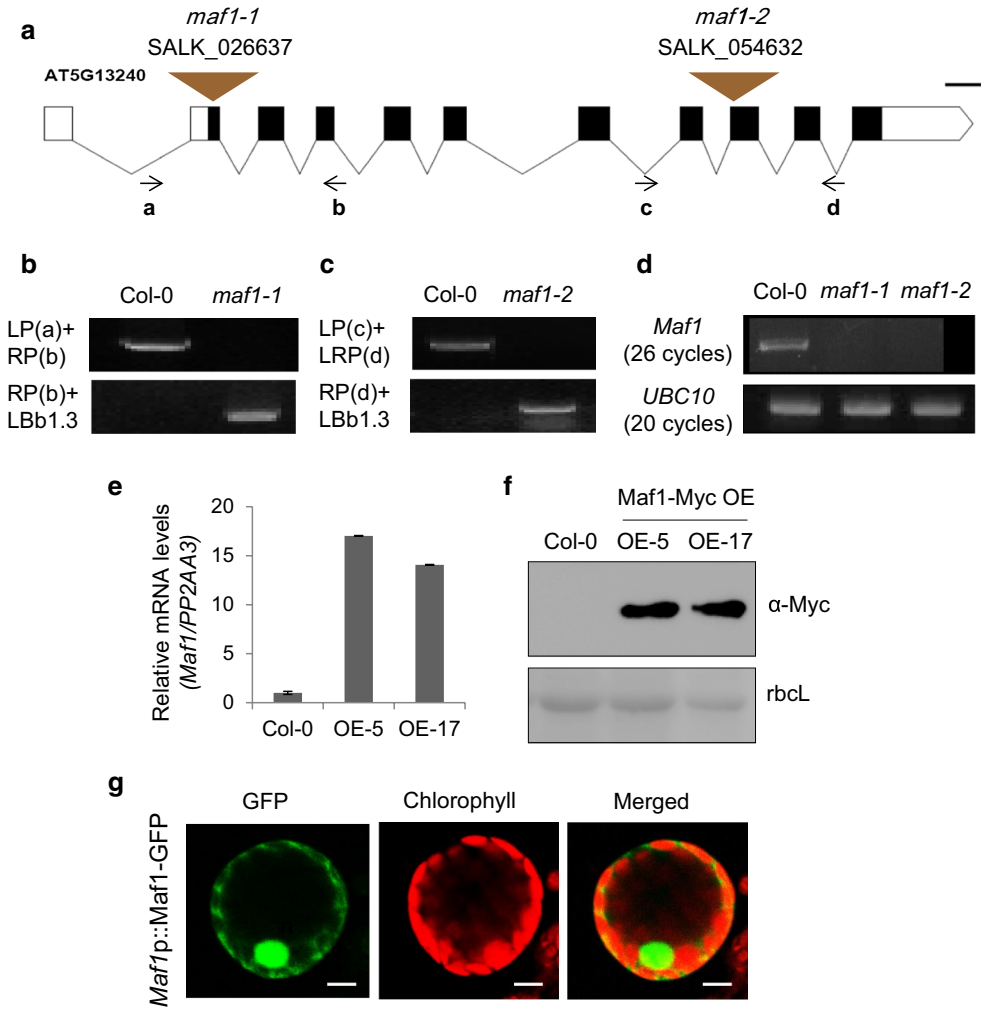

Fig. 1 Characterization of T-DNA insertion mutants of *Maf1* and *Maf1–Myc* overexpression lines. **a** Schematic presentation of T-DNA insertion sites in the *maf1* mutants, and locations of the primers used for genotyping. *Brown arrowheads* indicate T-DNA insertion sites of the *maf1-1* and *maf1-2* mutants. *Black arrows* indicate the location and orientation of each primer. Scale bar = 100 bp. **b**, **c** PCR-based genotyping of the *maf1-1* and *maf1-2* mutants. Three primers each were used for genotyping of the *maf1-1* **(b)** and *maf1-2* **(c)** mutants. The results suggest that the two mutant alleles are all homozygous. **d** RT-PCR analysis of *Maf1* expression in the *maf1-1* and *maf1-2* mutants. Primers and PCR cycle numbers are shown. *Maf1* primers detected the full-length *Maf1* mRNA. *UBC10* mRNA levels were used as controls. **e** RT-qPCR analysis of *Maf1* mRNA expression in Maf1–Myc OE-5 and OE-17 seedlings. Transcript levels were normalized by *PP2AA3* mRNA, and expressed relative to those in WT (Col-0). Error bars represent standard errors (SE) from three replications using 10-days-old seedling. **f** Immunoblotting with anti-Myc antibody to measure the expression of the Maf1–Myc fusion protein in WT (Col-0), OE-5, and OE-17 lines. Thirty micrograms of total protein isolated from seedlings were subjected to immunoblotting. Ponceau-stained rubisco large subunit (rbcL) was used as a loading control. **g** Subcellular localization of *Arabidopsis* Maf1. Maf1-GFP was transiently expressed under its own promoter (*Maf1*p::Maf1-GFP) in *N. benthamiana* leaves via agroinfiltration. GFP fluorescence in leaf protoplasts prepared from the infiltrated leaves was observed by confocal microscopy. *n*, nucleus. Scale bars = 20 µm

seedling morphology and chlorophyll contents (Fig. 2a, b). The fresh weight of the *maf1-1* and *maf1-2* mutant seedlings was also lower than that of WT seedlings after H_2O_2, MMS, and cisplatin treatments (Fig. S2a). These results suggest that Maf1 function is required for a plant's response to these stresses. In contrast, the Maf1–Myc OE seedlings did not show any visible morphological differences from WT seedlings, after the stress treatment (Fig. S1b).

The *maf1* mutants are more susceptible to the TOR inhibitor Torin-1

Since a functional link between Maf1 and the TOR pathway has been reported in yeast and mammals (Wei and Zheng 2010; Boguta 2012), we next examined the sensitivity of the *maf1-2* and *Maf1* OE-17 seedlings to Torin-1 compared with WT seedlings (Fig. 3a, b). Seedlings were grown for 7 days in 1/2 MS medium with 30 mM glucose

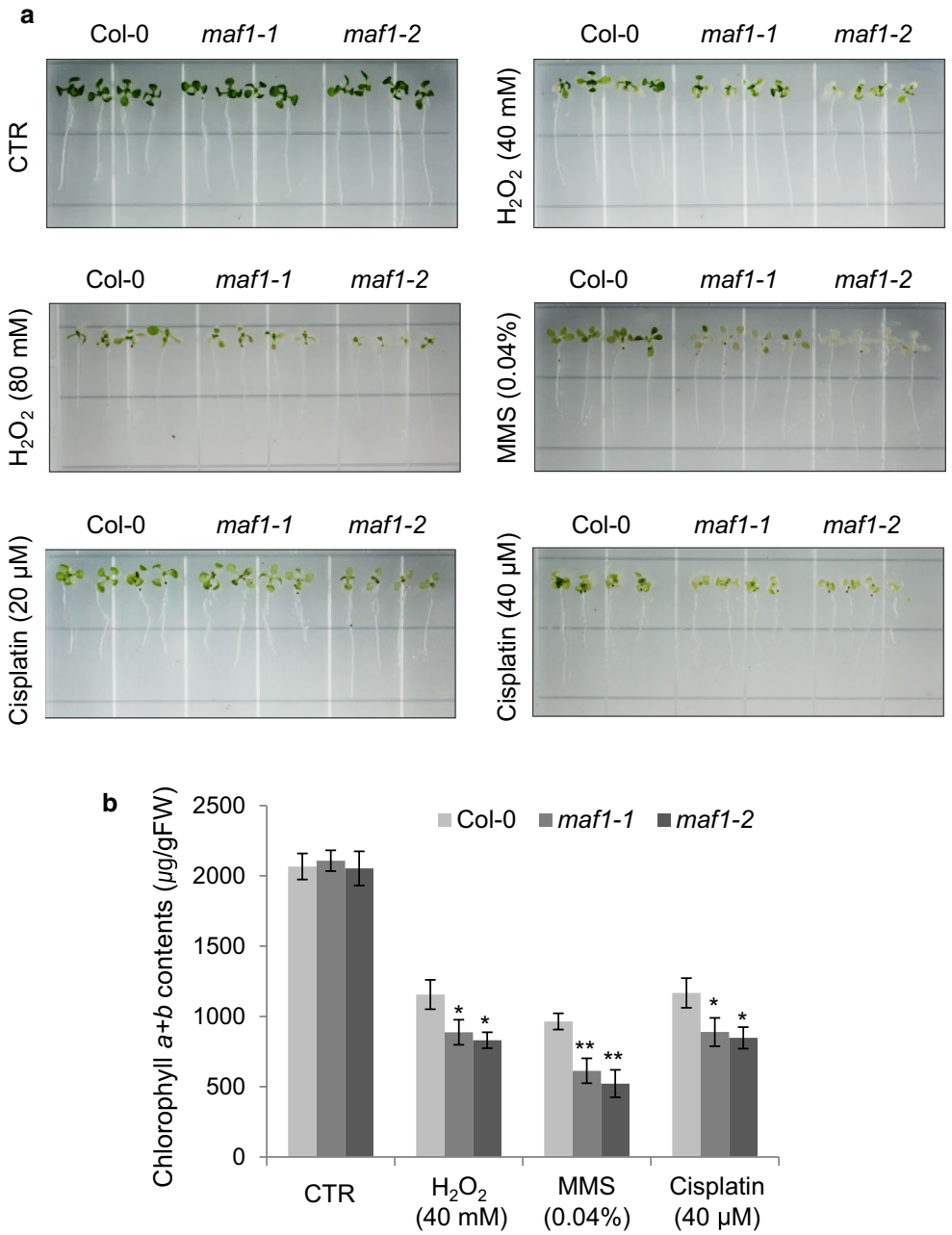

Fig. 2 Phenotypes and chlorophyll contents of the *maf1-1* and *maf1-2* mutant seedlings under stress conditions. **a** Seedlings grown for 7 days in liquid culture were incubated with H_2O_2 (40 and 80 mM) and MMS (0.04%) for 24 h, or with cisplatin (20 and 40 µM) for 48 h. Control seedlings (CTR) were grown without stress treatment for additional 48 h. **b** Total chlorophyll contents in the seedlings after stress treatment. Error bars represent SE from three biological replications using seedlings grown in different sets of liquid culture (*$P \leq 0.05$; **$P \leq 0.01$)

in the light (light and glucose condition; LG). They were then transferred to fresh medium with glucose for 3-day incubation in the light (LG) in the presence of 2, 4, and 8 µM Torin-1. Alternatively, the seedlings were transferred to medium without glucose for 3-day incubation in the dark (dark and starvation condition; DS) in the presence of 0.25 and 0.5 µM Torin-1. Torin-1 caused reduced growth and premature senescence in all of the seedlings, more strongly in DS than in LG. The *maf1-2* seedlings were more susceptible to Torin-1 than the WT and OE-17 seedlings, particularly under DS conditions (Fig. 3a). Accordingly, total chlorophyll contents in the *maf1-2* seedlings were consistently lower than those of the WT and OE-17 seedlings under all treatment conditions (Fig. 3b). Notably,

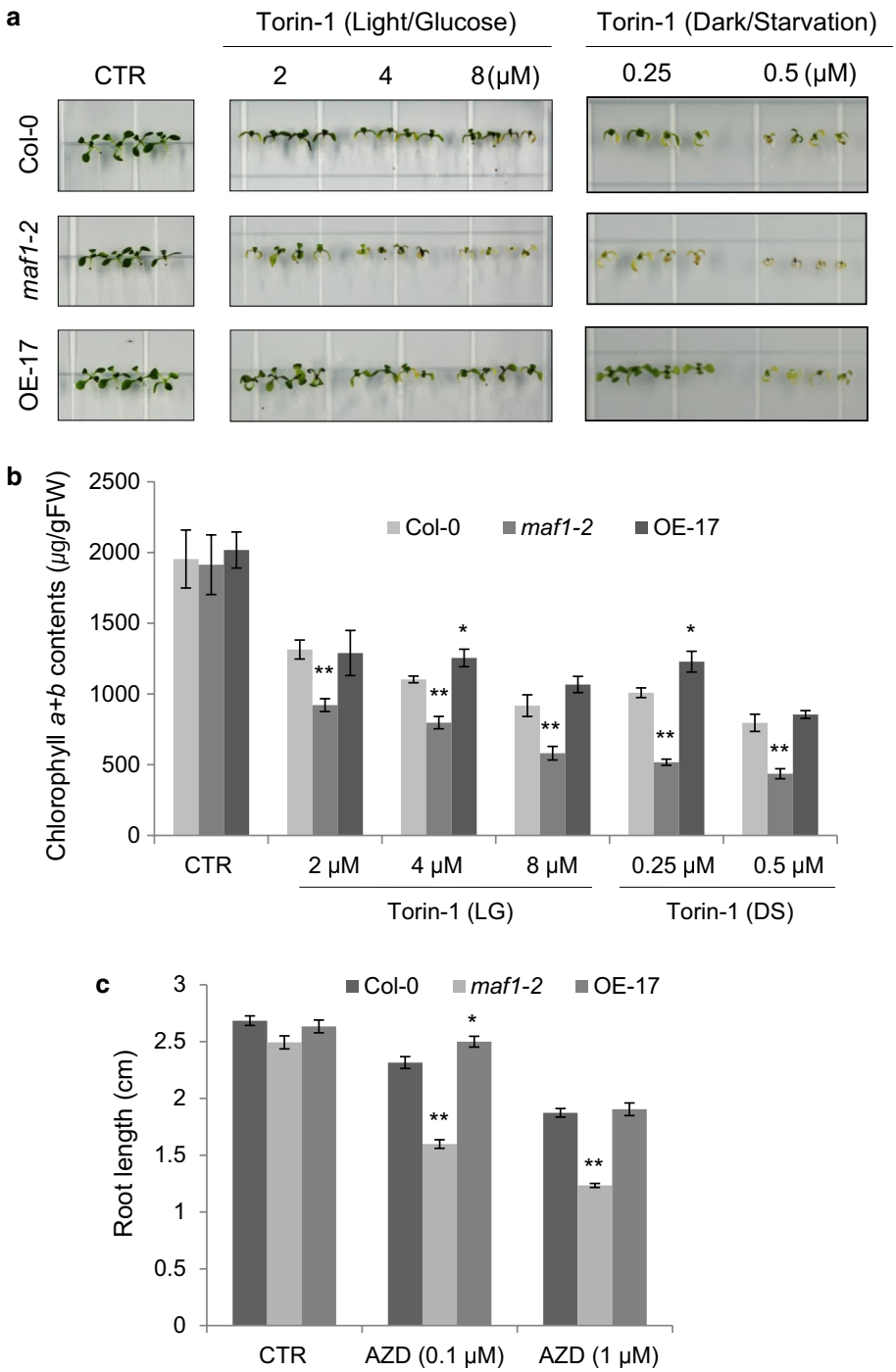

Fig. 3 Phenotypes and chlorophyll contents of the *maf1-2* mutant and the OE-17 seedlings after Torin-1 treatment. **a** Seedlings grown for 7 days in liquid culture were incubated with Torin-1 (2, 4, and 8 μM) under light/glucose conditions (LG), or with Torin-1 (0.25 and 0.5 μM) under dark/starvation conditions (DS) for 3 days. Control seedlings (CTR) were grown under normal conditions during the treatment time (3 days). **b** Total chlorophyll contents in the seedlings shown in **a**. Error bars represent SE from three biological replications using seedlings grown in different sets of liquid culture (*$P \leq 0.05$; **$P \leq 0.01$). **c** Root length of the seedlings was measured after treatment with AZD8055 (0.1 and 1 μM) for 3 days under LG conditions. Error bars represent SE from three biological replications using seedlings grown in different sets of liquid culture (*$P \leq 0.05$; **$P \leq 0.01$)

the OE-17 seedlings maintained higher chlorophyll contents under several Torin-1 treatment conditions. These results suggest that the *maf1-2* mutant and OE-17 seedlings show higher and slightly lower Torin-1 sensitivity than WT, respectively. Since root growth is sensitive to TOR inhibitors such as AZD8055 and Torin-1, we measured the root length of the *maf1-2* and OE-17 seedlings after 3 days of AZD8055 treatment (0.1 and 1 μM) under LG, compared with WT. Although AZD8055 caused reduced root growth in all seedlings, the *maf1-2* seedlings were clearly more susceptible to AZD8055 than the WT and OE-17 seedlings (Fig. 3c). Root length measurement also suggested that the *maf1-2* seedlings were more susceptible to Torin-1 (2 μM) than other seedlings after 3 and 5 days of treatment under LG conditions (Fig. S2b). The OE-17 seedlings exhibited slightly increased resistance to the TOR inhibitors under several treatment conditions (Figs. 3c, S2b).

Phosphorylation of Maf1 is regulated by cellular stresses

CsMAF1 is phosphorylated in vitro by several kinases of mammalian origin (Soprano et al. 2017). We examined whether Maf1 phosphorylation in vivo depends on cellular stress conditions using Phos-tag SDS-PAGE (Fig. 4a, b). Phos-tag specifically slows down the migration rate of phosphorylated proteins, causing band shifts in SDS-PAGE (Kinoshita et al. 2006, 2012). The Maf1–Myc OE-17 seedlings grown for 7 days in 1/2 MS liquid medium with 30 mM glucose were transferred to fresh medium without glucose (CTR) or fresh medium without glucose but containing H_2O_2 (40 mM), MMS (0.04%), or cisplatin (40 µM) for incubation for 24 h. We then performed Phos-tag SDS-PAGE using seedling extracts, followed by immunoblotting with anti-Myc antibody using Ponceau-stained rubisco large subunit (rbcL) as a loading control. The immunoblotting

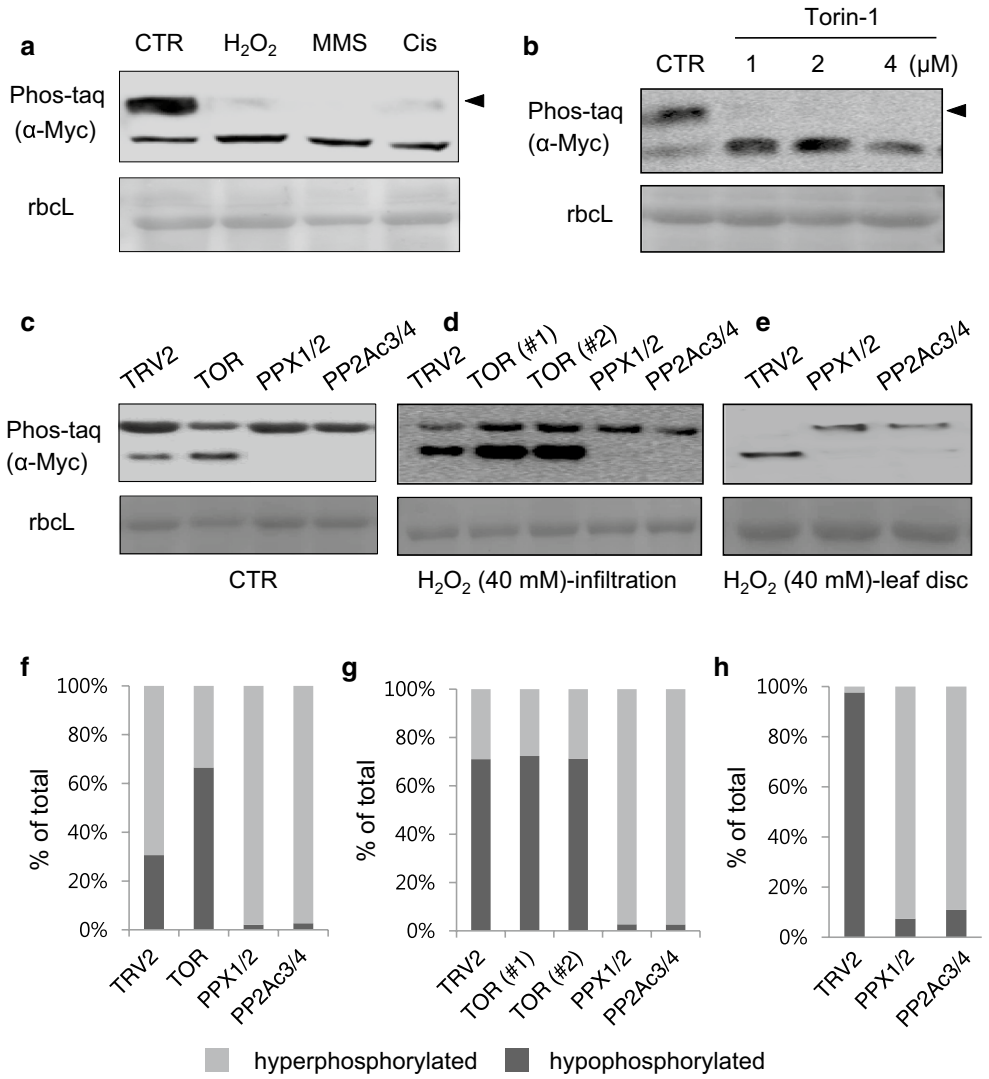

Fig. 4 Maf1 phosphorylation/dephosphorylation under stress conditions and its regulation by the TOR signaling pathway. **a** Maf1 dephosphorylation after diverse stress treatments. The Maf1–Myc OE-17 seedlings grown for 7 days in liquid culture were incubated with H_2O_2 (40 mM), MMS (0.04%), and cisplatin (40 µM) for 24 h. Control seedlings (CTR) were grown without stress treatment for additional 24 h. After treatment, total protein extracts from the seedlings were subjected to Zn^{2+}-Phostag SDS-PAGE, for immunoblotting with anti-Myc antibody. The hyperphosphorylated form of Maf1 is marked with the *arrowhead*. Ponceau-stained rbcL was used as a loading control. **b** Maf1 dephosphorylation after Torin-1 treatments. The OE-17 seedlings grown for 7 days in liquid culture were incubated with Torin-1 (1, 2, and 4 µM) for 3 days. Control seedlings (CTR) were grown under normal conditions during the treatment time (3 days). **c–e** Maf1 phosphorylation/dephosphorylation after VIGS of *TOR*, *PPX1/2* (PP4c), and *PP2Ac3/4* (PP2Ac) in the OE-17 plants. The plants were grown under normal conditions (**c**), infiltrated with H_2O_2 (**d**), or treated with H_2O_2 as leaf discs (**e**). **f–h** Quantification of the hyperphosphorylated and hypophosphorylated forms of Maf1 in each sample as a percentage of their total amount. Immunoblots shown in **c**, **d**, and **e** were quantified using Image J program in **f**, **g**, and **h**, respectively

detected two protein bands in the control sample (Fig. 4a). It has been reported that Maf1 is phosphorylated at multiple sites by multiple kinases including TOR kinase and Protein kinase A in citrus plants and mammals (Soprano et al. 2017). The upper band (marked with *arrowheads*) likely represents Maf1 proteins hyperphosphorylated at various sites, while the lower band represents hypophosphorylated Maf1. Previously, hyperphosphorylated Maf1 was detected as a shifted band at the upper position in yeast (Oficjalska-Pham et al. 2006; Towpik et al. 2008). Indeed, the calf intestinal alkaline phosphatase (CIP) treatment before Phos-tag SDS–PAGE caused mobility shift of the upper band to the lower position (Fig. S3), suggesting that the upper band represents the hyperphosphorylated form of Maf1. Based on the intensity of the upper and lower protein bands in the control seedlings, a large proportion of Maf1 was hyperphosphorylated under favorable conditions (Fig. 4a). However, stress treatments with H_2O_2, MMS, and cisplatin resulted in disappearance of the upper bands, suggesting that Maf1 becomes dephosphorylated in vivo under diverse stress conditions. Similarly, when the seedlings were treated with Torin-1 for 3 days under LG conditions, it also caused dephosphorylation of Maf1 proteins (Fig. 4b).

Virus-induced gene silencing (VIGS) of *TOR* and protein phosphatase genes

Next, we investigated whether Maf1 phosphorylation/dephosphorylation is modulated by the TOR signaling pathway. We performed VIGS in OE-17 plants using the tobacco rattle virus 2 (TRV2) system against several components of the TOR signaling pathway, including TOR kinase, protein phosphatase 4 catalytic subunits (PP4c), and PP2A catalytic subunits (PP2Ac). PP4 and PP2A belong to the PP2A family of phosphatases (Janssens and Goris 2001). For *TOR* silencing, a 649-bp cDNA fragment of *Arabidopsis TOR* was cloned into TRV2 vector as described (Lee et al. 2017). There are two genes, *PPX1* and *PPX2*, encoding PP4c in *Arabidopsis* (Pujol et al. 2000). To silence both *PPX1* and *PPX2* genes, a 585-bp cDNA fragment of *PPX1* was inserted into the TRV2 vector (PPX1/2 VIGS). *PPX2* would likely be silenced by the *PPX1* sequence in the construct due to high nucleotide sequence identity (92%) between the two genes. Among the five catalytic subunit isoforms in *Arabidopsis* (Farkas et al. 2007), PP2Ac3 and PP2Ac4 (subfamily II) are mainly and redundantly involved in the control of plant growth and development (Ballesteros et al. 2013; Spinner et al. 2013). The subfamily I isoforms (PP2Ac1, PP2Ac2, and PP2Ac5) appeared to play a role in plant defense response (He et al. 2004). Thus, we decided to perform VIGS against *PP2Ac3* and *PP2Ac4* genes. A 590-bp cDNA fragment of *PP2Ac3* was cloned into TRV2 vector for simultaneous silencing of *PP2Ac3* and *PP2Ac4* (PP2Ac3/4 VIGS). The nucleotide sequence identity between *PP2Ac3* and *PP2Ac4* was 91%. All VIGS constructs were transformed into *Agrobacterium*, and VIGS was performed in the OE-17 seedlings using agroinfiltration as described in "Materials and methods".

VIGS of *TOR* caused defective plant growth and premature senescence at ~ 15 days after infiltration (DAI), associated with a reduction in *TOR* mRNA levels to approximately 12% of the TRV2 control levels (Fig. S4a, b). VIGS using the *PPX1* construct reduced the *PPX1* and *PPX2* transcript levels to approximately 18% of the TRV2 control, based on RT-qPCR using primers recognizing both genes (Fig. S4c). However, the *PPX1/2* VIGS plants showed no visible phenotypic changes under normal growth conditions despite repeated attempts (Fig. S4a). Kataya et al. (2017) reported that knockout mutant lines of *PPX1* and *PPX2* were unavailable, and furthermore, their knockdown transgenic lines could not be generated. We speculate that it may require more severe silencing of *PPX1* and *PPX2* to yield VIGS phenotypes. The *PP2Ac3/4* VIGS plants displayed growth retardation with round, thick leaves in the shoot apical regions (Fig. S4a). The inflorescence stems of the plants were characteristically short and thick (results not shown). These vegetative phenotypes were consistent with those of the *pp2ac3-c4* double mutations with leaky *pp2ac3* alleles (Spinner et al. 2013). RT-qPCR analyses using primers detecting both genes showed that *PP2Ac3* and *PP2Ac4* mRNA levels decreased to 46% of the TRV2 control levels after *PP2Ac3/4* VIGS (Fig. S4d). VIGS against *TOR*, *PPX1/2*, and *PP2Ac3/4* resulted in the same phenotypes in both OE-17 and WT (Col-0) plants.

Phosphorylation of Maf1 is regulated by TOR and protein phosphatases

To investigate whether TOR, PP4c, and PP2Ac subfamily II play a role in phosphorylation/dephosphorylation of Maf1, we performed Phos-tag SDS–PAGE using leaf extracts of diverse VIGS plants grown under normal conditions (CTR), followed by immunoblotting with anti-Myc antibody (Fig. 4c). The band intensity of the immunoblot was quantified using Image J program (Fig. 4f). TRV2 control plants displayed similar band patterns of hyperphosphorylated and hypophosphorylated Maf1, compared to those of the OE-17 seedlings under normal conditions (Fig. 4a, c). Quantification revealed that the hyperphosphorylated and hypophosphorylated forms were approximately 68% and 32% of total Maf1, respectively. *TOR* silencing increased the percentage of the lower hypophosphorylated form of Maf1 to 65%, while it, accordingly, reduced the percentage of the upper hyperphosphorylated form to 35% (Fig. 4c, f). This result suggests that reduced TOR activity leads to Maf1 dephosphorylation. In contrast, the lower hypophosphorylated form

of Maf1 almost disappeared in *PPX1/2* and *PP2Ac3/4* VIGS samples, suggesting that both PP4 and PP2A activities are critical for Maf1 dephosphorylation (Fig. 4c, f).

We next investigated the involvement of TOR, PP4c, and PP2Ac subfamily II in phosphorylation/dephosphorylation of Maf1 under stress conditions. Leaves of the VIGS plants (15 DAI) were infiltrated with 40 mM H_2O_2, and after 24 h, the leaf extracts were subjected to Phos-tag SDS-PAGE and immunoblotting (Fig. 4d, g). H_2O_2 treatment reversed the ratio of hyperphosphorylated and hypophosphorylated Maf1 in TRV2 plants, compared to that under normal conditions; the hyperphosphorylated and hypophosphorylated forms were 29% and 71% of the total Maf1 proteins, respectively. This result suggests that Maf1 becomes dephosphorylated under the stress conditions. Silencing of *TOR* under the stress conditions slightly increased the proportion of the hypophosphorylation form to 70–72% in two different samples of harvested leaves (Fig. 4d, g). Silencing of *PPX1/2* or *PP2Ac3/4* under the stress conditions did not further change the phosphorylation/dephosphorylation patterns of Maf1 (Fig. 4d, g). Furthermore, when leaf discs made from TRV2, PPX1/2, and PP2Ac3/4 VIGS plants were floated on 40 mM H_2O_2 solution for 24 h, Maf1 was completely hypophosphorylated in TRV2 control, but mostly hyperphosphorylated in *PPX1/2*- or *PP2Ac3/4*-silenced cells (Fig. 4e, h). These results collectively suggest the importance of TOR and PP4/PP2A phosphatases for Maf1 phosphorylation and dephosphorylation, respectively.

Maf1 interacts with PP4 and PP2A catalytic subunits in the nucleus under stress conditions

To determine whether Maf1 interacts with PP4c and PP2Ac under control and stress conditions, we performed bimolecular fluorescence complementation (BiFC) (Fig. 5a). Maf1 was expressed as YFP^N-fusion protein in combination with PPX1, PPX2, PP2Ac3, and PP2Ac4 as YFP^C-fusion proteins in *N. benthamiana* leaves by agroinfiltration. At 30 h after agroinfiltration, leaves were infiltrated with H_2O_2 (40 mM), MMS (0.04%), or cisplatin (40 μM). After 16 h, leaves were harvested and protoplasts were generated for observation using confocal microscopy. There was no yellow fluorescence in protoplasts under normal conditions. However, H_2O_2, MMS, and cisplatin treatments yielded yellow fluorescence in the nucleus of the leaf protoplasts in every combination, suggesting that Maf1 stably interacts with PPX1, PPX2, PP2Ac3, and PP2Ac4 in the nucleus under the stress conditions (Fig. 5a).

Next, we performed co-immunoprecipitation assays under control and stress conditions (Fig. 5b, c). Myc-tagged Maf1 and Flag-tagged PPX1 or PP2Ac3 were expressed in *N. benthamiana* leaves using agroinfiltration. Stress treatments with H_2O_2 (40 mM), MMS (0.04%), or cisplatin (40 μM) were carried out as described in Fig. 5a. Expression of Maf1–Myc, PPX1-Flag, and PP2Ac3-Flag was detected by immunoblotting using anti-Myc or anti-Flag antibodies (input). PPX1-Flag and PP2Ac3-Flag were immunoprecipitated from leaf extracts using anti-Flag antibody-conjugated resin (IP), followed by immunoblotting with anti-Myc antibody to detect co-immunoprecipitated Maf1–Myc protein. Maf1–Myc was co-immunoprecipitated with PPX1-Flag and PP2Ac3-Flag proteins under the stress conditions, but not under control conditions (Fig. 5b, c), which is consistent with the BiFC results (Fig. 5a). Collectively, these results suggest that Maf1 stably interacts with PP4c and PP2Ac in the nucleus under diverse stress conditions.

The *maf1* mutations increase cellular levels of 5S RNA and pre-tRNAs under stress conditions

As a Pol III repressor, Maf1 represses transcription of 5S rDNA and tRNA genes in yeast and mammals (Upadhya et al. 2002; Reina et al. 2006; Goodfellow et al. 2008; Boguta 2012). In plants, *CsMAF1* silencing and overexpression, respectively, increased and decreased the cellular levels of several pre-tRNAs under normal growth conditions (Soprano et al. 2013). However, Maf1 target RNA expression under stress conditions has not been examined in plants. The WT (Col-0), *maf1-1*, and *maf1-2* seedlings grown in liquid culture were treated with H_2O_2 (40 mM) or MMS (0.04%) for 24 h, or with cisplatin (20 μM) for 48 h. To examine the effects of Maf1 deficiency on Maf1 target gene expression, RT-qPCR was performed using total RNA isolated from untreated seedlings (CTR) and the stress-treated seedlings, with primers recognizing 5S rRNA, pre-$tRNA^{His}$, pre-$tRNA^{Thr}$, and pre-$tRNA^{Leu}$ (Fig. 6a–d). Based on RT-qPCR, the four RNAs were more abundantly detected in the *maf1-1* and *maf1-2* seedlings than in the WT seedlings under both normal (Fig. 6a) and stress conditions (Fig. 6b–d). Particularly, expression of 5S rRNA and the pre-tRNAs was highly upregulated after cisplatin treatment in the *maf1* mutants, compared with the WT (Fig. 6d).

Silencing of *TOR* and protein phosphatase genes affects the expression of Maf1 target RNAs

Since phosphorylation/dephosphorylation of Maf1 is modulated by TOR and PP4/PP2A phosphatases, we tested if silencing of *TOR*, *PPX1/2*, and *PP2Ac3/4* affects expression of Maf1 target RNAs. We performed RT-qPCR analyses using total RNA isolated from leaves of the TRV2, TRV2:PPX1/2, and TRV2:PP2Ac3/4 VIGS plants or WT plants (Col-0), all of which were grown under normal conditions (CTR). Silencing of *PPX1/2* and *PP2Ac3/4* increased cellular levels of pre-$tRNA^{His}$, pre-$tRNA^{Thr}$,

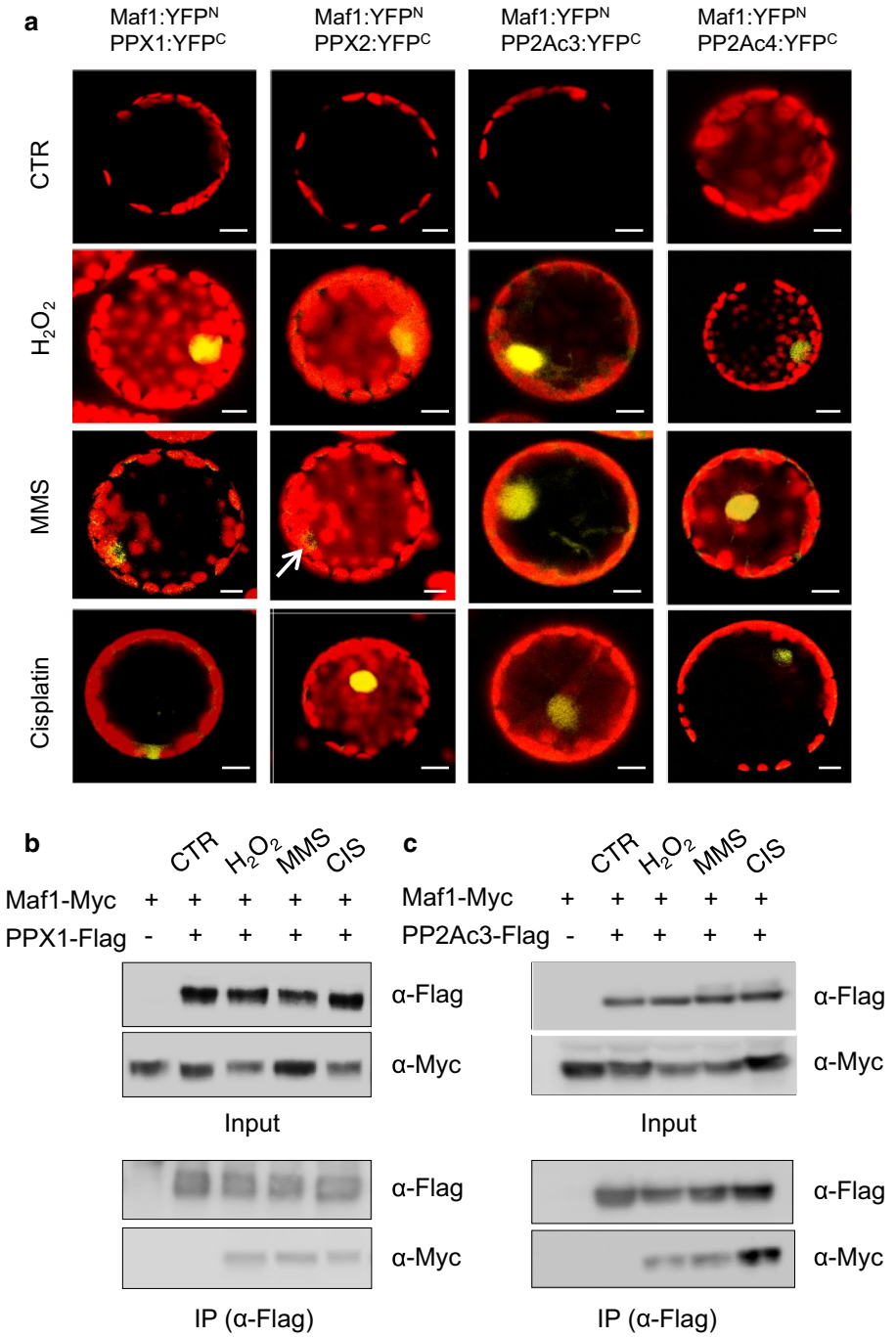

Fig. 5 Maf1 interactions with PP4c and PP2Ac under normal and stress conditions. **a** Bimolecular fluorescence complementation (BiFC). YFP^N- and YFP^C-fusion proteins were co-expressed in *N. benthamiana* leaves by agroinfiltration. Then the leaves were infiltrated with H_2O_2 (40 mM), MMS (0.04%), and cisplatin (40 µM). After 16 h, leaf protoplasts were observed by confocal microscopy. The *white arrow* indicates the yellow fluorescence in the nucleus. Scale bars = 20 µm. **b**, **c** Co-immunoprecipitation of Maf1 with PPX1 (**b**) and PP2Ac3 (**c**). Maf1–Myc and PPX1-Flag (**b**), or Maf1–Myc and PP2Ac3-Flag (**c**) were co-expressed in *N. benthamiana* leaves by agroinfiltration. Then the leaves were infiltrated with H_2O_2 (40 mM), MMS (0.04%), and cisplatin (40 µM). After stress treatment, total protein extracts were immunoprecipitated with anti-Flag antibody-conjugated resin, and the co-immunoprecipitate was detected using the anti-Myc antibody

and pre-$tRNA^{Leu}$, compared with that of TRV2 control or WT (Fig. 6e). In contrast, silencing of *TOR* significantly downregulated the expression of 5S rRNA, pre-$tRNA^{His}$, pre-$tRNA^{Thr}$, and pre-$tRNA^{Leu}$ in two different samples of harvested leaves, compared with the TRV2 control (Fig. 6f). Thus, dephosphorylation status of Maf1 in TOR-, PP4c-, and PP2Ac-deficient plants is correlated with its target RNA expression.

Discussion

Maf1 encodes a Pol III repressor, evolutionarily conserved from plants to mammals. In this study, we investigated plant Maf1 functions under diverse stress conditions using *Arabidopsis maf1* mutants. We also explored mechanisms of Maf1 phosphorylation/dephosphorylation by components of the TOR signaling pathway including TOR, PP4

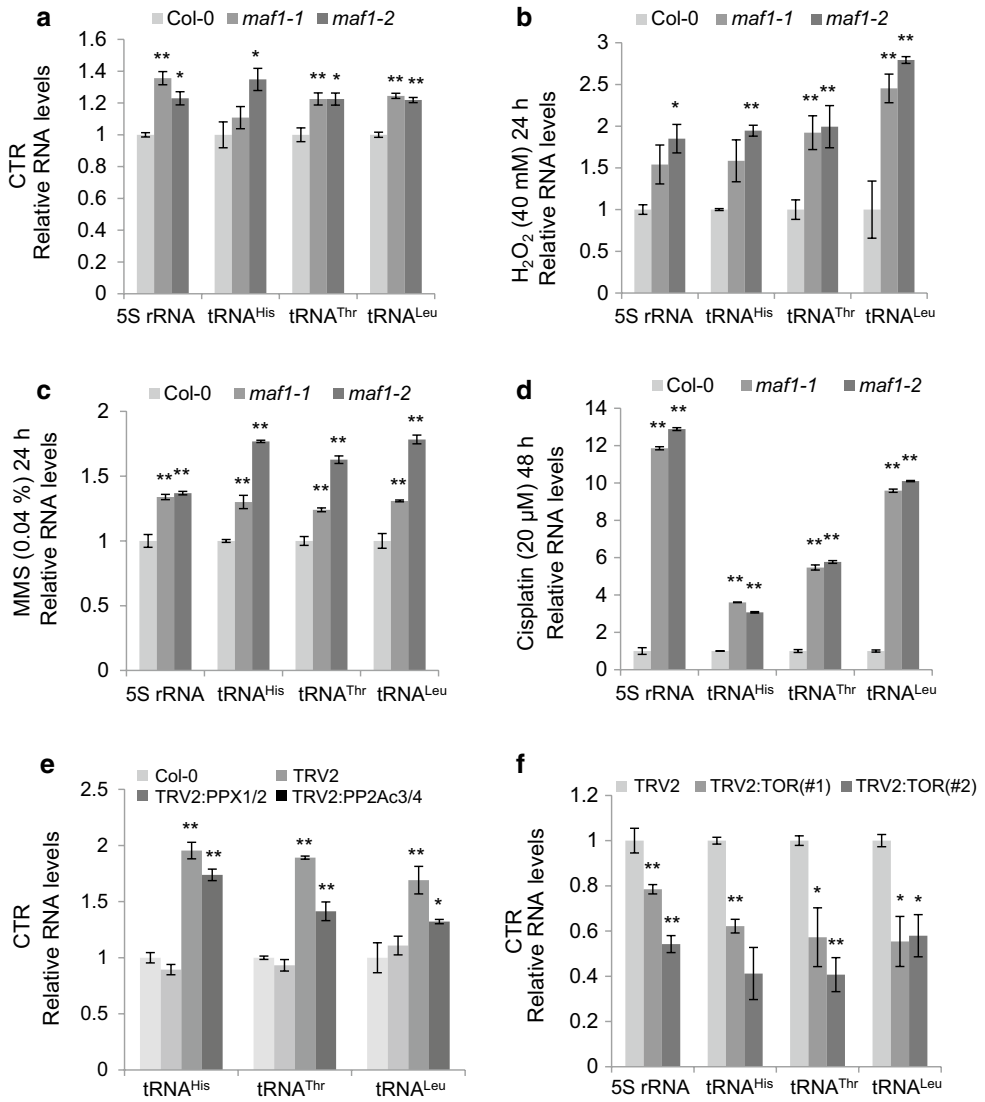

Fig. 6 Maf1 target gene expression in the *maf1* mutants and VIGS plants. **a–d** RT-qPCR analyses of 5S rRNA, pre-tRNA^{His}, pre-tRNA^{Thr}, and pre-tRNA^{Leu} levels in the WT (Col-0), and the *maf1-1* and *maf1-2* mutants. The seedlings grown for 7 days in liquid culture were incubated with H_2O_2 (40 mM) (**b**) and MMS (0.04%) (**c**) for 24 h, or with cisplatin (20 μM) for 48 h (**d**). Control seedlings (CTR) were grown without stress treatment for additional 48 h (**a**). After treatment, total RNA was isolated and RT-qPCR was performed. Transcript levels were normalized by *PP2AA3* mRNA, and expressed relative to those in the WT (Col-0). Error bars represent SE from three biological replications using seedlings grown in different sets of liquid culture (*$P \leq 0.05$; **$P \leq 0.01$). **e** RT-qPCR analyses of pre-tRNA^{His}, pre-tRNA^{Thr}, and pre-tRNA^{Leu} levels in PPX1/2 and PP2Ac3/4 VIGS plants. Error bars represent SE from three biological replications using the 9th and 10th leaves collected from three VIGS plants for each replication (*$P \leq 0.05$; **$P \leq 0.01$). **f** RT-qPCR analyses of 5S rRNA, pre-tRNA^{His}, pre-tRNA^{Thr}, and pre-tRNA^{Leu} levels in TOR (#1) and TOR (#2) VIGS plants. Transcript levels were normalized by *PP2AA3* mRNA, and expressed relative to those of TRV2 control (*$P \leq 0.05$; **$P \leq 0.01$)

and PP2A. The *maf1* mutations caused hypersensitivity to diverse stresses, including H_2O_2 (oxidative stress), MMS (DNA damaging stress), and cisplatin (replication stress), and to the TOR inhibitors AZD8055 and Torin-1 (Figs. 2, 3). These results suggest that Maf1 function is critical to a plant's adaptation to diverse stresses. Since the cost of tRNA synthesis is high, transcription of tRNA genes is suppressed immediately when environmental conditions become adverse (Boguta and Graczyk 2011). As a global Pol III repressor, Maf1 constitutes a controlling mechanism that coordinates cellular Pol III activity with fluctuating environmental conditions in yeast and mammals (Wei and Zheng 2010; Boguta and Graczyk 2011; Boguta 2012). In this study, increased susceptibility of *maf1* mutants to diverse stresses suggests that rapid repression of 5S RNA and tRNA transcription by Maf1 may be critical for the conservation of cellular energy and resources under stress conditions in plants. Since recent studies in

yeast suggested that Maf1 is indirectly involved in tRNA processing and degradation (Boguta and Graczyk 2011; Karkusiewicz et al. 2011; Turowski et al. 2012), other defects in tRNA metabolism may have contributed to the susceptibility of the mutants.

Although Maf1 is the unique global regulator of Pol III-mediated transcription in yeast, both *maf1*-Δ mutants and Maf1 OE yeast cells showed normal growth under standard conditions (Boguta et al. 1997; Pluta et al. 2001; Oler and Cairns 2012). In this study, the *Arabidopsis maf1* mutations caused no visible growth defect under normal conditions. Thus, Maf1 functions appear to be dispensable in favorable cell environment in both *Arabidopsis* and yeast. Maf1 overexpression (OE) in *Arabidopsis* resulted in slightly increased resistance to the TOR inhibitors (Fig. 3), without visibly affecting plant growth or plant's response to H_2O_2, MMS, and cisplatin (Fig. S1). The OE-5 and OE-17 plants contained moderately reduced levels of 5S rRNA and the pre-tRNAs under normal conditions (Fig. S5), suggesting that the high *Maf1* transcript levels in the OE plants (Fig. 1e) caused only a mild increase in Maf1 repressor activity. There are several possible explanations; excessive Maf1 proteins may be inactivated by hyperphosphorylation or degraded by proteasomes using multiple ubiquitylation motifs within Maf1, or modulated by both processes. Previously, to observe Maf1 OE phenotypes in citrus plants, etiolated sweet orange epicotyls were transformed with *Agrobacterium* containing the 35Sp::CsMAF1 construct, which were then grafted onto *Citrus limonia* root stocks for shoot development (Soprano et al. 2017). Most of the shoots that emerged from the epicotyls showed growth arrest and premature senescence symptoms. These results suggest that Maf1 OE may be detrimental to shoot growth, particularly in certain culture conditions.

Studies in yeast and mammals have established that phosphorylation/dephosphorylation control is the key mechanism of Maf1 regulation (Boguta and Graczyk 2011; Boguta 2012). Maf1 is inactivated by phosphorylation in favorable conditions, while unfavorable growth conditions and rapamycin induce dephosphorylation of Maf1 by protein phosphatases. The rapid Pol III repression was correlated with Maf1 dephosphorylation in yeast and mammals, and furthermore, any mutations that impair Maf1 dephosphorylation disturbed the repression (Reina et al. 2006; Goodfellow et al. 2008; Kantidakis et al. 2010; Michels et al. 2010). In plants, recombinant CsMAF1 protein was phosphorylated in vitro by PKA and TOR kinase of mammalian origin (Soprano et al. 2017). However, in vivo phosphorylation status of plant Maf1 under normal and stress conditions has not been determined. Using Phos-tag gels, we have shown that Maf1 is mostly hyperphosphorylated in vivo under normal conditions, but becomes dephosphorylated upon diverse stresses and Torin-1 treatment (Fig. 4). Thus, under stress conditions, protein phosphatase activity appears to dominate over kinase activity, producing hypophosphorylated Maf1 as an active repressor of Pol III. It has been shown that Maf1 is phosphorylated at multiple sites by multiple kinases in plants, yeast, and mammals. Our Phos-tag SDS-PAGE analyses could not separate each Maf1 form in different phosphorylation status; they detected two protein bands, the hyperphosphorylated and hypophosphorylated Maf1 forms, in different proportions depending on the conditions. Furthermore, Maf1 deficiency elevated Pol III target gene expression under both normal and stress conditions, particularly upon cisplatin treatment (Fig. 6a–d), supporting Maf1's function as the Pol III repressor.

To identify the TOR components that affect Maf1 phosphorylation in vivo, we performed Phos-tag SDS-PAGE using the Maf1–Myc OE-17 plants after VIGS of *TOR*, *PPX1/2* (PP4c), and *PP2Ac3/4* (PP2Ac subfamily II), with and without H_2O_2 treatment. *TOR* silencing stimulated Maf1 dephosphorylation under normal conditions (Fig. 4c, f), consistent with the result upon Torin-1 treatment (Fig. 4b), but did not significantly increase Maf1 dephosphorylation above the level that normally occurred under stress conditions (Fig. 4d, g). These results suggest that TOR itself and/or other kinases under the control of TOR mediate Maf1 phosphorylation in vivo. The finding by Soprano et al. (2017) that CsMAF1 is phosphorylated by mTOR in vitro supports that TOR kinase phosphorylates Maf1 in plants. Furthermore, our analyses suggested that both PP4 and PP2A phosphatases are critically involved in Maf1 dephosphorylation. This finding differs from that in yeast; PP4 is the main enzyme for Maf1 dephosphorylation in yeast to couple stress conditions to Pol III repression (Oler and Cairns 2012). It is well known that TOR kinase regulates PP4 and PP2A in yeast in response to diverse stimuli (Duvel and Broach 2004; Di Como and Jiang 2006). In plants, Tap46, the TOR signaling component and the regulatory subunit of PP2A family phosphatases, interacts with the catalytic subunits of PP4 and PP2A (Ahn et al. 2011, 2015a). PP4 has been implicated in plant growth, miRNA processing, and DNA damage response, via the analyses of their regulatory subunits (Kataya et al. 2017; Su et al. 2017). PP2A is involved in various cellular processes in plants, such as phytohormone signaling (Michniewicz et al. 2007; Tang et al. 2011; Waadt et al. 2015), light signaling (Tseng and Briggs 2010), and cytoskeleton organization (Kirik et al. 2012; Spinner et al. 2013). The observation that expression of Pol III target RNAs decreased and increased upon *TOR* silencing and *PP4c/PP2Ac* silencing, respectively (Fig. 6e, f) reveals the correlation between Maf1 repressor activity and its dephosphorylation status.

Arabidopsis Maf1 was localized predominantly in the nucleus, but was also detected in the cytosol (Fig. 1g), consistent with the localization of CsMAF1 (Soprano et al.

2017). Interestingly, leaf disc excision causes CsMAF1-GFP accumulation in the nucleolus, although a significant part of the fusion protein is still found in the nucleoplasm. We did not consistently observe Maf1 transport from the nucleoplasm to the nucleolus under the tested stress conditions. Furthermore, BiFC and co-immunoprecipitation suggested that Maf1 interacts with the catalytic subunits of PP4 and PP2A in the nucleus, under the stress conditions (Fig. 5). These results suggest that Maf1 protein becomes dephosphorylated predominantly in the nucleus in response to the stresses. A further study is required to understand the mechanism and physiological importance of Maf1 trafficking between the nucleoplasm and the nucleolus in plants. We failed to detect stable interactions between Maf1 and PP4c/PP2Ac under normal conditions (Fig. 5). However, *PPX1/2* and *PP2Ac3/4* VIGS caused a reduction in Maf1 dephosphorylation in normal conditions, accompanied by elevated expression of pre-tRNAs (Figs. 4c, 6e). These results suggest that PP4 and PP2A may still dephosphorylate Maf1 in normal conditions, but their interactions may be relatively weak. Maf1 activity is likely kept in balance by activation and inactivation of Maf1 kinases and phosphatases in fluctuating cell environments of plants. The interplay between various Maf1 kinases and phosphatases under different growth conditions should be investigated in the future.

Author contribution statement CSA designed and performed all the experiments with the help of D-HL. CSA and H-SP discussed the results and wrote the manuscript.

Acknowledgements This research was supported by the Cooperative Research Program for Agriculture Science and Technology Development [Project numbers PJ013212 (PMBC) and PJ013227 (SSAC)] from the Rural Development Administration, and Mid-Career Researcher Program (NRF-2016R1A2B4013180) from the National Research Foundation (NRF) of the Republic of Korea.

Compliance with ethical standards

Conflict of interest The authors declare no conflict of interest.

References

Ahn CS, Han JA, Lee HS, Lee S, Pai HS (2011) The PP2A regulatory subunit Tap46, a component of the TOR signaling pathway, modulates growth and metabolism in plants. Plant Cell 23:185–209

Ahn CS, Ahn HK, Pai HS (2015a) Overexpression of the PP2A regulatory subunit Tap46 leads to enhanced plant growth through stimulation of the TOR signalling pathway. J Exp Bot 66:827–840

Ahn HK, Kang YW, Lim HM, Hwang I, Pai H-S (2015b) Physiological functions of the COPI complex in higher plants. Mol Cells 38:866–875

Apel K, Hirt H (2004) Reactive oxygen species: metabolism, oxidative stress, and signal transduction. Annu Rev Plant Biol 55:373–399

Ballesteros I, Domínguez T, Sauer M, Paredes P, Duprat A, Rojo E, Sanmartín M, Sánchez-Serrano JJ (2013) Specialized functions of the PP2A subfamily II catalytic subunits PP2A-C3 and PP2A-C4 in the distribution of auxin fluxes and development in *Arabidopsis*. Plant J 73:862–872

Bögre L, Henriques R, Magyar Z (2013) TOR tour to auxin. EMBO J 32:1069–1071

Boguta M (2012) Maf1, a general negative regulator of RNA polymerase III in yeast. Biochim Biophys Acta 1829:376–384

Boguta M, Graczyk D (2011) RNA polymerase III under control: repression and de-repression. Trends Biochem Sci 36:451–456

Boguta M, Czerska K, Zoladek T (1997) Mutation in a new gene *MAF1* affects tRNA suppressor efficiency in *Saccharomyces cerevisiae*. Gene 185:291–296

Boisnard S, Lagniel G, Garmendia-Torres C, Molin M, Boy-Marcotte E, Jacquet M, Toledano MB, Labarre J, Chedin S (2009) H_2O_2 activates the nuclear localization of Msn2 and Maf1 through thioredoxins in *Saccharomyces cerevisiae*. Eukaryot Cell 8:1429–1438

Burch-Smith TM, Schiff M, Liu Y, Dinesh-Kumar SP (2006) Efficient virus-induced gene silencing in *Arabidopsis*. Plant Physiol 142:21–27

Clough SJ, Bent AF (1998) Floral dip: a simplified method for Agrobacterium-mediated transformation of *Arabidopsis thaliana*. Plant J 16:735–743

Desai N, Lee J, Upadhya R, Chu Y, Moir RD, Willis IM (2005) Two steps in Maf1-dependent repression of transcription by RNA polymerase III. J Biol Chem 280:6455–6462

Di Como CJ, Jiang Y (2006) The association of Tap42 phosphatase complexes with TORC1: another level of regulation in Tor signaling. Cell Cycle 5:2729–2732

Dieci G, Fiorino G, Castelnuovo M, Teichmann M, Pagano A (2007) The expanding RNA polymerase III transcriptome. Trends Genet 23:614–622

Dobrenel T, Caldana C, Hanson J, Robaglia C, Vincentz M, Veit B, Meyer C (2016) TOR signaling and nutrient sensing. Annu Rev Plant Biol 67:261–285

Duvel K, Broach J (2004) The role of phosphatases in TOR signaling in yeast. Curr Top Microbiol Immunol 279:19–38

Farkas I, Dombradi V, Miskei M, Szabados L, Koncz C (2007) *Arabidopsis* PPP family of serine/threonine phosphatases. Trends Plant Sci 12:169–176

Gately DP, Howell SB (1993) Cellular accumulation of the anticancer agent cisplatin: a review. Brit J Cancer 67:1171–1176

Goodfellow SJ, Graham EL, Kantidakis T, Marshall L, Coppins BA, Oficjalska-Pham D, Gérard M, Lefebvre O, White RJ (2008) Regulation of RNA polymerase III transcription by Maf1 in mammalian cells. J Mol Biol 378:481–491

Graczyk D, Debski J, Muszynska G, Bretner M, Lefebvre O, Boguta M (2011) Casein kinase II-mediated phosphorylation of general repressor Maf1 triggers RNA polymerase III activation. Proc Natl Acad Sci USA 108:4926–4931

Hannan KM, Brandenburger Y, Jenkins A et al (2003) mTOR-dependent regulation of ribosomal gene transcription requires S6K1 and is mediated by phosphorylation of the carboxy-terminal activation domain of the nucleolar transcription factor UBF. Mol Cell Biol 23:8862–8877

He X, Anderson JC, del Pozo O, Gu YQ, Tang X, Martin GB (2004) Silencing of subfamily I of protein phosphatase 2A catalytic subunits results in activation of plant defense responses and localized cell death. Plant J 38:563–577

Janssens V, Goris J (2001) Protein phosphatase 2A: a highly regulated family of serine/threonine phosphatases implicated in cell growth and signalling. Biochem J 353:417–439

Kantidakis T, Ramsbottom BA, Birch JL, Dowding SN, White RJ (2010) mTOR associates with TFIIIC, is found at tRNA and 5S

rRNA genes, and targets their repressor Maf1. Proc Natl Acad Sci USA 107:11823–11828
Karkusiewicz I, Turowski TW, Graczyk D, Towpik J, Dhungel N, Hopper AK, Boguta M (2011) Maf1 protein, repressor of RNA polymerase III, indirectly affects tRNA processing. J Biol Chem 286:39478–39488
Kataya ARA, Creighton MT, Napitupulu TP, Saetre C, Heidari B, Ruoff P, Lillo C (2017) PLATINUM SENSITIVE 2 LIKE impacts growth, root morphology, seed set, and stress responses. PLoS One 12:e0180478
Kinoshita E, Kinoshita-Kikuta E, Takiyama K, Koike T (2006) Phosphate-binding tag, a new tool to visualize phosphorylated proteins. Mol Cell Proteomics 5:749–757
Kinoshita E, Kinoshita-Kikuta E, Koike T (2012) Phos-tag SDS–PAGE systems for phosphorylation profiling of proteins with a wide range of molecular masses under neutral pH conditions. Proteomics 12:192–202
Kirik A, Ehrhardt DW, Kirik V (2012) TONNEAU2/FASS regulates the geometry of microtubule nucleation and cortical array organization in interphase *Arabidopsis* cells. Plant Cell 24:1158–1170
Lee J, Moir RD, Willis IM (2009) Regulation of RNA polymerase III transcription involves SCH9-dependent and SCH9-independent branches of the target of rapamycin (TOR) pathway. J Biol Chem 284:12604–12608
Lee DH, Park SJ, Ahn CS, Pai HS (2017) MRF family genes are involved in translation control, especially under energy-deficient conditions, and their expression and functions are modulated by the TOR signaling pathway. Plant Cell 29:2895–2920
Lundin C, North M, Erixon K, Walters K, Jenssen D, Goldman AS, Helleday T (2005) Methyl methanesulfonate (MMS) produces heat-labile DNA damage but no detectable in vivo DNA double-strand breaks. Nucleic Acids Res 33:3799–3811
Ma XM, Blenis J (2009) Molecular mechanisms of mTOR-mediated translational control. Nat Rev Mol Cell Biol 10:307–318
Mayer C, Grummt I (2006) Ribosome biogenesis and cell growth: mTOR coordinates transcription by all three classes of nuclear RNA polymerases. Oncogene 25:6384–6391
Michels AA, Robitaille AM, Buczynski-Ruchonnet D, Hodroj W, Reina JH, Hall MN, Hernandez N (2010) mTORC1 directly phosphorylates and regulates human MAF1. Mol Cell Biol 30:3749–3757
Michniewicz M, Zago MK, Abas L et al (2007) Antagonistic regulation of PIN phosphorylation by PP2A and PINOID directs auxin flux. Cell 130:1044–1056
Moir RD, Lee J, Haeusler RA, Desai N, Engelke DR, Willis IM (2006) Protein kinase A regulates RNA polymerase III transcription through the nuclear localization of Maf1. Proc Natl Acad Sci USA 103:15044–15049
Oficjalska-Pham D, Harismendy O, Smagowicz W et al (2006) General repression of RNA polymerase III transcription is triggered by protein phosphatase type 2A-mediated dephosphorylation of Maf1. Mol Cell 22:623–632
Oler AJ, Cairns BR (2012) PP4 dephosphorylates Maf1 to couple multiple stress conditions to RNA polymerase III repression. EMBO J 31:1440–1452
Pluta K, Lefebvre O, Martin NC, Smagowicz WJ, Stanford DR, Ellis SR, Hopper AK, Sentenac A, Boguta M (2001) Maf1p, a negative effector of RNA polymerase III in *Saccharomyces cerevisia*e. Mol Cell Biol 21:5031–5040
Porra RJ, Scheer H (2000) 18O and mass spectrometry in chlorophyll research: Derivation and loss of oxygen atoms at the periphery of the chlorophyll macrocycle during biosynthesis, degradation and adaptation. Photosynth Res 66:159–175
Pujol G, Baskin TI, Casamayor A, Cortadellas N, Ferrer A, Ariño J (2000) The Arabidopsis thaliana PPX/PP4 phosphatases: molecular cloning and structural organization of the genes and immunolocalization of the proteins to plastids. Plant Mol Biol 44:499–511
Reina JH, Azzouz TN, Hernandez N (2006) Maf1, a new player in the regulation of human RNA polymerase III transcription. PLoS One 1:e134
Revenkova E, Masson J, Koncz C, Afsar K, Jakovleva L, Paszkowski J (1999) Involvement of *Arabidopsis thaliana* ribosomal protein S27 in mRNA degradation triggered by genotoxic stress. EMBO J 18:490–499
Roberts D, Wilson B, Huff J, Stewart A, Cairns B (2006) Dephosphorylation and genome-wide association of Maf1 with Pol III-transcribed genes during repression. Mol Cell 22:633–644
Rollins J, Veras I, Cabarcas S, Willis I, Schramm L (2007) Human Maf1 negatively regulates RNA polymerase III transcription via the TFIIB family members Brf1 and Brf2. Int J Biol Sci 3:292–302
Schepetilnikov M, Dimitrova M, Mancera-Martinez E, Geldreich A, Keller M, Ryabova LA (2013) TOR and S6K1 promote translation reinitiation of uORF-containing mRNAs via phosphorylation of eIF3h. EMBO J 32:1087–1102
Soprano AS, Abe VY, Smetana JH, Benedetti CE (2013) Citrus MAF1, a repressor of RNA polymerase III, binds the *Xanthomonas citri* canker elicitor PthA4 and suppresses citrus canker development. Plant Physiol 163:232–242
Soprano AS, Giuseppe PO, Shimo HM et al (2017) Crystal structure and regulation of the citrus Pol III repressor MAF1 by auxin and phosphorylation. Structure 25:1360–1370
Spinner L, Gadeyne A, Belcram K et al (2013) A protein phosphatase 2A complex spatially controls plant cell division. Nat Commun 4:1863
Su C, Li Z, Cheng J, Li L, Zhong S, Liu L, Zheng Y, Zheng B (2017) The protein phosphatase 4 and SMEK1 complex dephosphorylates HYL1 to promote miRNA biogenesis by antagonizing the MAPK cascade in *Arabidopsis*. Dev Cell 41:527.e5–539.e5
Tang W et al (2011) PP2A activates brassinosteroid-responsive gene expression and plant growth by dephosphorylating BZR1. Nat Cell Biol 13:124–131
Thoreen CC, Chantranupong L, Keys HR, Wang T, Gray NS, Sabatini DM (2012) A unifying model for mTORC1-mediated regulation of mRNA translation. Nature 485:109–113
Towpik J, Graczyk D, Gajda A, Lefebvre O, Boguta M (2008) Derepression of RNA polymerase III transcription by phosphorylation and nuclear export of its negative regulator, Maf1. J Biol Chem 283:17168–17174
Tseng TS, Briggs WR (2010) The *Arabidopsis rcn1-1* mutation impairs dephosphorylation of Phot2, resulting in enhanced blue light responses. Plant Cell 22:392–402
Turowski TW, Karkusiewicz I, Kowal J, Boguta M (2012) Maf1-mediated repression of RNA polymerase III transcription inhibits tRNA degradation via RTD pathway. RNA 18:1823–1832
Upadhya R, Lee J, Willis IM (2002) Maf1 is an essential mediator of diverse signals that repress RNA polymerase III transcription. Mol Cell 10:1489–1494
Vannini A, Ringel R, Kusser AG, Berninghausen O, Kassavetis GA, Cramer P (2010) Molecular basis of RNA polymerase III transcription repression by Maf1. Cell 143:59–70
Waadt R, Manalansan B, Rauniyar N et al (2015) Identification of open stomata1-interacting proteins reveals interactions with sucrose non-fermenting1-related protein kinases2 and with type 2A protein phosphatases that function in abscisic acid responses. Plant Physiol 169:760–779
Wei Y, Zheng XFS (2010) Maf1 regulation: a model of signal transduction inside the nucleus. Nucleus 1:162–165
Wei Y, Tsang CK, Zheng XF (2009) Mechanisms of regulation of RNA polymerase III-dependent transcription by TORC1. EMBO J 28:2220–2230

White RJ (2008) RNA polymerases I and III, non-coding RNAs and cancer. Trends Genet 24:622–629

Wullschleger S, Loewith R, Hall MN (2006) TOR signaling in growth and metabolism. Cell 124:471–484

Xiong Y, Sheen J (2013) Moving beyond translation: glucose-TOR signaling in the transcriptional control of cell cycle. Cell Cycle 12:1989–1990

Zaragoza D, Ghavidel A, Heitman J, Schultz MC (1998) Rapamycin induces the G0 program of transcriptional repression in yeast by interfering with the TOR signaling pathway. Mol Cell Biol 18:4463–4470